Marine Pollution Bulletin 159 (2020) 111483

Contents lists available at ScienceDirect

Marine Pollution Bulletin

journal homepage: www.elsevier.com/locate/marpolbul

Formation and fate of oil-related aggregates (ORAs) in seawater at different temperatures

Ingrid A. Henry, Roman Netzer, Emlyn J. Davies, Odd Gunnar Brakstad*

SINTEF Ocean AS, Environment and New Resources, Trondheim, Norway

ARTICLE INFO

Keywords:
Marine snow
Dispersed oil
Microbial communities
Biodegradation
Aggregation
Sinking

ABSTRACT

In this study, the formation and fate of oil-related aggregates (ORAs) from chemically dispersed oil in seawater (SW) were investigated at different temperatures (5 °C, 13 °C, 20 °C). Experiments in natural SW alone, and in SW amended with typical marine snow constituents (phytoplankton and mineral particles), showed that the presence of algae stimulated the formation of large ORAs, while high SW temperature resulted in faster aggregate formation. The ORAs formed at 5 °C and 13 °C required mineral particles for sinking, while the aggregates also sank in the absence of mineral particles at 20°. Early in the experimental periods, oil compound accumulation in ORAs was faster than biodegradation, particularly in aggregates with algae, followed by rapid biodegradation. High abundances of bacteria associated with hydrocarbon biodegradation were determined in the ORAs, together with algae-associated bacteria, while clustering analyses showed separation between bacterial communities in experiments with oil alone and oil with algae/mineral particles.

1. Introduction

Marine snow (MarS) formation is a natural process in the marine environment, transporting particulate organic carbon to the deep waters. These macroscopic particles are mainly made up of detritus, living organisms and inorganic material. The particles are “glued” together by sticky polymers, termed transparent exopolymer particles (TEP), mainly produced by diatoms (Alldredge and Silver, 1988; De La Rocha and Passow, 2007), but also bacteria producing extracellular polymeric substance (EPS) may be involved (Bhaskar and Bhosle, 2005). Several laboratory and field studies have shown large variations in MarS sinking velocities, ranging from 1 to > 350 m/day (Alldredge and Silver, 1988).

During the Deepwater Horizon (DWH) accident in the Gulf of Mexico (GoM) in 2010, there was a focus on potential oil sedimentation caused by oil-related aggregates (ORAs) associated with MarS-related processes, suggested to be caused primarily by fall-out from the deep-sea plume, but sedimentation was also suggested to originate from surfaced oil (Stout and Payne, 2016; Valentine et al., 2014). Small aggregates were detected in the deep-sea plume, as well as in oil incubation experiments with seawater (SW) from the GoM, containing materials associated with proteins, carbohydrates, alkanes and degradation products (Bælum et al., 2012; Hazen et al., 2010). Several attempts were made to estimate the amounts of sedimented oil, ranging from approximately 80,000 to 620,000 barrels (Chanton et al., 2014; Stout et al., 2017; Valentine et al., 2014). However, these estimates did not include the significant oil weathering caused by dissolution and biodegradation before and after sedimentation (Bagby et al., 2017; Stout and Payne, 2016; Yergeau et al., 2015). Since the oil spill site was not far from the Mississippi delta, and the river outflow became strong during the spill period, suspended sediment transported by the river was also likely to interact with oil and contribute to oil sinking (Kourafalou and Androulidakis, 2013; Vonk et al., 2015).

Experimental studies with high oil concentrations have shown that ORAs from field-collected or laboratory-prepared oil samples resulted in oil sedimentation, although also floating aggregates were observed (Passow and Ziervogel, 2016; Passow et al., 2012). Both oil-degrading bacteria, suspended particles and oil-diatom coagulation seemed to be involved in the ORA formation processes (Passow et al., 2012). These experiments also indicated that the use of chemical dispersants resulted in the inhibition of ORA formations at high dispersant concentrations, and it was suggested that the dispersant constituents also dispersed the particulate exopolymers required for the aggregation (Passow et al., 2017; Passow and Ziervogel, 2016). However, chemically prepared oil dispersions and dispersants will rapidly dilute in the SW column (Lee et al., 2013).

It has also been suggested that ORA processes have been important in other oil spills than DWH (Vonk et al., 2015). However, research on

* Corresponding author at: SINTEF Ocean AS, Postboks 4762, Torgarden, 7465 Trondheim, Norway.
E-mail address: odd.g.brakstad@sintef.no (O.G. Brakstad).

https://doi.org/10.1016/j.marpolbul.2020.111483
Received 13 March 2020; Received in revised form 21 June 2020; Accepted 13 July 2020
Available online 24 July 2020

ORA processes from other regions than the GoM, and particularly from colder water, is limited (Netzer et al., 2018). In the studies described here, we have investigated ORA processes in natural SW at three different temperatures, with focus on aggregate formation, microbial community successions, oil compound biodegradation and aggregate sinking behaviour. The selected SW temperatures represented summer (13 °C) and winter (5 °C) conditions in temperate regions, and these temperatures were compared to warmer SW (20 °C) more relevant for southern latitudes. Since chemical dispersants were used as a major oil spill response method during the DWH spill, and the use of these chemicals has proven to increase oil biodegradation (Brakstad et al., 2014; Bælum et al., 2012; McFarlin et al., 2014; Prince et al., 2013; Siron et al., 1995; Techtmann et al., 2017; Venosa and Holder, 2007), we used chemically dispersed oil in the experiments.

2. Materials and methods

2.1. Oils, dispersants and seawater

A fresh Norwegian naphthenic crude oil (Troll C) was used in this study (density of 0.900, pour point of −18 °C, asphaltene content of 0.2 wt%, and wax content of 2.0 wt%). The oil was heated prior to use (50 °C, 1 h) to melt wax generated during storage. Corexit 9500A (Nalco Environmental Solutions LLC, Suger Land, Tx, USA) was used as dispersant in the study.

Natural SW was collected from a depth of 80 m (below thermocline) in a Norwegian fjord (Trondheimsfjord; 63°26′N, 10°23′E), outside the harbour area of Trondheim. The SW is continuously supplied via a pipeline system to our laboratories, after passing through a sand filter. The SW source is considered to be non-polluted and not influenced by seasonal variations, with a salinity of 34‰.

2.2. Phytoplankton and mineral particles

The obligate marine psychrophilic diatom *Fragilariopsis cylindrus* RCC 4289 (Roscoff Culture Collection, Roscoff Cedex, France), with reported cell length 15–20 μm, diameter 3–4 μm (http://nordicmicroalgae.org), was selected for cold SW experiments at 5 °C. The diatom culture was grown at 5 °C, as recently described (Netzer et al., 2018). The marine diatom *Skeletonema pseudocostatum* NIVA-BAC (NIVA Culture Collection, Oslo, Norway), with reported cell length 2–61 μm and diameter 2–21 μm (http://nordicmicroalgae.org), was used in experiments in temperate and warm water at 13 °C and 20 °C, respectively. The *P. pseudocostatum* culture was grown at 20 °C, as described (ISO 10253, 2016). Algal growth was monitored by cell counting in a Bürker haemocytometer, using light microscopy at 400 times magnification. Cells from the stationary-state phase were used for the experiments, and concentrations determined by the Bürker haemocytometer analyses were used to dilute to final concentrations.

Commercially available diatomaceous earth (Celite 512, Sigma-Aldrich), median size 16 μm (information from the supplier) was used as mineral particles in experiments at temperate and warm water conditions.

2.3. Microcosm set-up experiments for biodegradation studies

Oil was premixed at room temperature at a dispersant-to-oil ratio (DOR) of 1:100. Stock dispersions of oil were then prepared in filtered (1 μm) natural non-amended SW, using an oil droplet generator, consisting of 3 chambers connected by nozzles. Oil dispersions with defined oil droplet size distributions and concentrations are generated by injecting oil via a capillary into a flow of seawater which moves through the chambers (Nordtug et al., 2011) Stock dispersions were prepared at concentrations of 200 mg/L and with median oil droplet sizes of ~10 μm in the droplet generator. Oil concentrations and droplet sizes were determined by Coulter Counter (Multisizer 4, Beckman Coulter Inc., Brea, CA, USA).

Pyrex flasks (2 L; Schott) were baked (450 °C; 3 h) and soaked overnight (4% Deconex 11 Universal, Borer, Switzerland), washed with detergent (Neodisher N, Dr. Weigert, Germany), and thoroughly rinsed and autoclaved (121 °C, 20 min). The flasks were then filled with natural unamended SW, which was acclimated for 48 h at the experimental temperatures (5°, 13°, or 20 °C). Approximately 50 mL headspaces were left in the flasks for stock solutions of oil dispersion, diatoms and mineral particles. Stock dispersions of oil were applied at final concentrations of 15 mg/L (experiments at 13 °C and 20 °C) or 30 mg/L (experiment at 5 °C). Diatom cultures of *F. cylindrus* (5 °C) or *S. pseudocostatum* (13 °C and 20 °C) were counted (Bürker haemocytometer) and then applied in final nominal concentrations of 10,000 cells/mL at all temperatures. Celite was applied at a final concentration of 5 mg/L. Experimental set-ups are shown in Supplementary information (Table S1). All flasks were then completely filled with SW acclimated at respective temperatures. Sterilized controls were included, using filtered (0.2 μm) SW supplied by 100 mg/L $HgCl_2$. The flasks were incubated in the dark in a low-energy carousel system consisting of wheels slowly rotating around the carousel axis (0.75 r.p.m.) by a gear motor (Brakstad et al., 2015) in temperature-controlled rooms (5, 13, or 20 °C) for up to 28 (13 °C and 20 °C) or 64 (5 °C) days.

2.4. Sampling

Triplicate samples were sacrificed for analysis after 0 day on the carousel (30 min on carousel), and then after 5, 21 and 64 days at 5 °C, after 5, 10, 19 and 32 days at 13 °C, and after 5, 9, 20 and 28 days at 20 °C, as described in Table S1. Sterilized controls (one replicate each) were sampled at day 0 and at the last day of each experiment. Particles in the oil dispersions with a diameter > 20 μm were defined as oil-related aggregates (ORAs) in the experiments (Netzer et al., 2018). Sampling was performed by sacrificing the contents of the entire flasks at the corresponding sampling time point (Table S1). Oil droplet concentrations and size distributions (range of 2–60 μm droplets sizes) were analysed in the Multisizer Coulter Counter (100 μm aperture), while dissolved oxygen (DO) was determined by a DO meter (Model 59 Dissolved Oxygen Meter, YSI Inc., Yellow Springs, OH, USA). The rest of the sample volume (2.2 L) was carefully filtered through a 20 μm steel filter mesh (Teichhansel Teichshop/Siebgewebeshop; Bockhorn, Germany) using gravimetric force to capture ORAs. Biofilm attached to the glass wall was released by careful shaking prior to filtration. The steel filter was then divided into two equal parts using sterilized scissors, one half of the filter was extracted in 20 mL dichloromethane (DCM) for chemical analyses, while the other half was frozen for subsequent DNA extraction from the ORAs. Planktonic bacteria were collected by filtering 500 mL of the flow-through (filtrate) from the first filtration-step through a 0.22 μm membrane filter by using a vacuum pump. The membrane filter was frozen at −20 °C for subsequent DNA extraction. The rest of the flow-through (approximately 1.7 L) was acidified with 15% HCl to pH < 2 and subjected to solvent-solvent extraction with DCM. The glass wall of each flask was washed with DCM to remove attached oil compounds, and the DCM extract was mixed with the extract of the flow-through from the same flask.

2.5. Chemical analyses

Oil analyses of DCM extracts in the ORAs and the water phases were performed by gas chromatographic methods. A gas chromatograph coupled to a flame ionization detector (GC-FID; Agilent 6890 N with 30 mDB1 column; Agilent Technologies) was used for quantification of C10-C36 total extractable organic material (TEOM). Targeted analytes were quantified in a gas chromatograph coupled to a mass spectrometer (GC–MS; Agilent 6890 plus GC coupled with an Agilent 5973 MSD detector, operated in Selected Ion Monitoring [SIM] modus; Agilent Technologies). GC–MS analyses included *n*C10-*n*C36 alkanes, the

isoprenoids pristane and phytane, decalins (C10-saturates), phenols, 2- to 6-ring polycyclic aromatic hydrocarbons (PAH) and 17α(H),21β(H)-hopane (30ab hopane), as previously described (Brakstad et al., 2014, 2015). Target compounds were normalized against 30ab hopane (Prince et al., 1994), or pristane/phytane (Atlas and Bartha, 1992).

2.6. Nucleic acid extraction and 16 rDNA amplicon analyses

DNA from biomass trapped on steel filters (ORAs) and membrane filters (planktonic bacteria) was extracted by FastDNA Spin kit for soil (MP Biomedicals) in combination with the FastPrep machine (MP Biochemicals), according to the manufacturer's instructions. DNA quantification was performed by Qubit 3.0 fluorometer (Thermo Fisher Scientific, Waltham, MA, USA) using the dsDNA High Sensitivity kit (Thermo Fisher Scientific). Microbial community compositions (covering Bacteria and Archaea) of the samples collected were analysed by 16S amplicon sequencing (Illumina MiSeq), as recently described (Netzer et al., 2018). DNA sequencing was performed by the University of Bielefeld, Bielefeld, Germany, or Macrogen, Inc., Seoul, South-Korea.

16S rDNA amplicons were generated from DNA-samples by two PCR rounds with the 2× HiFi HotStart ReadyMix (Kapa Biosystems, Boston MA, USA). For the first PCR round, the primers 341F (5′CCTAYGGG-RBGCASCAG) and 806R (5′GGACTACNNGGGTATCTAAT), covering both the domains Bacteria and Archaea were used to amplify the third and fourth variable regions (V3, V4) of the 16S rRNA gene (Yu et al., 2005). In the second round, the sequencing adapters and multiplexing indices where added using the Nextera XT Index kit (Illumina). Following each PCR round, amplicons were purified using the QIAquick PCR purification Kit (Qiagen) and finally the amplicon size and concentration were determined on a BioAnalyzer (Agilent Technologies, Santa Clara, CA, USA). DNA libraries were pooled, normalized (4 pM DNA) and mixed with PhiX (5%) Control v3 (Illumina), denatured at 96 °C for 2 min and run on a MiSeq sequencer (Illumina) using the MiSeq Reagent Kit v3 in the 2 × 300 bp paired-end mode.

Demultiplexed sequence data were received from Macrogen or Bielefeld in FASTQ format and imported into the QIIME2 v2019.4 version of the QIIME software (Bolyen et al., 2019) for analysis. Assembled sequences were denoised, filtered and trimmed to remove low quality reads (median quality score fell below 20), with the DADA2 plugin (Callahan et al., 2016). Amplicon sequences were aligned (Katoh and Toh, 2010; Stackebrandt and Goodfellow, 1991) and classified within QIIME2 using the SILVA v132 database (Quast et al., 2013) with a classifier trained on the amplified region (Bokulich et al., 2018). Next, the biome file was generated and used as input for R Phyloseq package v.1.12.2 (McMurdie and Holmes, 2013) for beta diversity and community composition analysis. Statistical analyses were performed within the Phyloseq package v.1.12.2 (McMurdie and Holmes, 2013) in R-studio v.3.6.2. The sequencing depth of individual samples is given in Fig. S8 (Supplementary information).

To analyze potential differences in the dynamics of microbial communities between individual samples and sample groups at separate time points, multivariate statistics in the form of principal coordinate analysis (PCoA), based on Bray-Curtis dissimilarity was carried out (Schroeder and Jenkins, 2018). For illustrating the taxonomical composition replicates were merged and a cut-off of 5% relative abundance was applied. Taxa below this threshold were assigned to the group “Other”.

2.7. SilCam analyses

The SilCam measurements of ORA settling velocities within a settling column were recorded at 15 Hz and pairs of images analysed together, whereby each particle was tracked from one frame to another (Davies et al., 2017; Brakstad et al., 2020).

Paired *t*-test analyses were performed by GraphPad Prism version 6.1 (GraphPad Software, San Diego, CA, USA). First-order rate coefficients and half-lives were determined by non-linear regression analyses by GraphPad Prism (options “One-phase decay” or “Plateau followed by one-phase decay”).

2.8. Sinking velocity experiment

A separate sinking velocity experiment of ORAs was performed in natural SW with a mixture of premixed (Corexit, DOR 1:100) oil dispersion (15 mg/L, ~10 μm droplet size) and algae (*S. pseudocostatum*, 10,000 cells/ml), oil dispersion and Celite (5 mg/L), oil dispersion, algae and Celite, or oil dispersion alone. The different mixtures were incubated in flat 1 L Pyrex flasks (completely filled) in the carousel system and incubated at 20 °C for 8–9 days. Aggregate formation was monitored with a silhouette camera (SINTEF SilCam) to document changes insize distribution for particles > 100 μm. Images are acquired in colour at 15 Hz for about 60 s for each sample (Davies et al., 2017). After incubation, the content of each flask was carefully transferred to a sinking chamber with a 1 m long settling column (Supplementary information Fig. S1), as recently described (Brakstad et al., 2020). In brief, the settling columns and an upper chamber above the columns were filled with natural SW from the same source as used in the treatments. The system was temperature-acclimated at 20 °C overnight in at temperature-controlled room to hold the same temperature as in the treatments. Flasks with aggregates were then carefully inverted while submerged in the upper chamber and mounted in the screw-cap in the top of the column, to avoid turbulence in the system (Fig. S1). Sinking velocities were measured in the bottom of the column by the SilCam system.

3. Results and discussions

3.1. ORA formation

Since ORA formation has mainly been associated with oil, mucus-producing bacteria and diatoms, and inorganic particles, we performed the experiments in the presence of these components. While the bacterial source was natural local SW, diatom species included the obligate psychrophilic diatom *F. cylindrus* (Netzer et al., 2018), and *S. pseudocostatum*, which is a cosmopolitan diatom (Kooistra et al., 2008). Both diatom species are producers of TEP associated with MarS formation (Aslam et al., 2012; Engel, 2000). In the initial experiments, which were performed at 5 °C, oil concentrations of 30 mg/L were used, but later experiments at the higher temperatures (13 °C and 20 °C) showed similar aggregate formation also at lower oil concentrations, and 15 mg/L oil was therefore used at these temperatures.

Dispersed oil was generated in the experiments by the oil droplet generator (Nordtug et al., 2011), resulting in an overall median oil droplet size of 9.3 ± 1.1 μm. During the low temperature experiment at 5 °C, no SilCam analyses were performed. However, visible observations showed that aggregation became apparent after 21 days of incubation at this temperature, as previously reported (Netzer et al., 2018). SilCam analyses at incubations of 13° and 20 °C showed that increasing aggregate sizes were observed by time in all incubations, and particularly in the presence of algae (Fig. 1). The aggregates reached median sizes > 2000 μm during incubations at both 13 °C and 20 °C (Fig. 1), with the largest aggregates in the presence of algae after 3–4 weeks of incubation (3220 ± 1797 μm after 21 days of incubation at 13 °C and 2760 ± 1607 μm after 28 days of incubation at 20 °C; Figs. 1, S2, Supplementary information). The occurrences of aggregates were accompanied by a reduction in turbidity, which could be related to a considerable reduction in oil droplet concentrations in all incubations (Fig. S3, Supplementary information), while median free oil droplet sizes (not integrated in the ORAs) remained within ranges of 8–12 μm in dispersions without diatoms or mineral particles (results not shown). The reduced oil droplet concentrations therefore coincided well with the aggregate formations in experiments with oil and diatoms

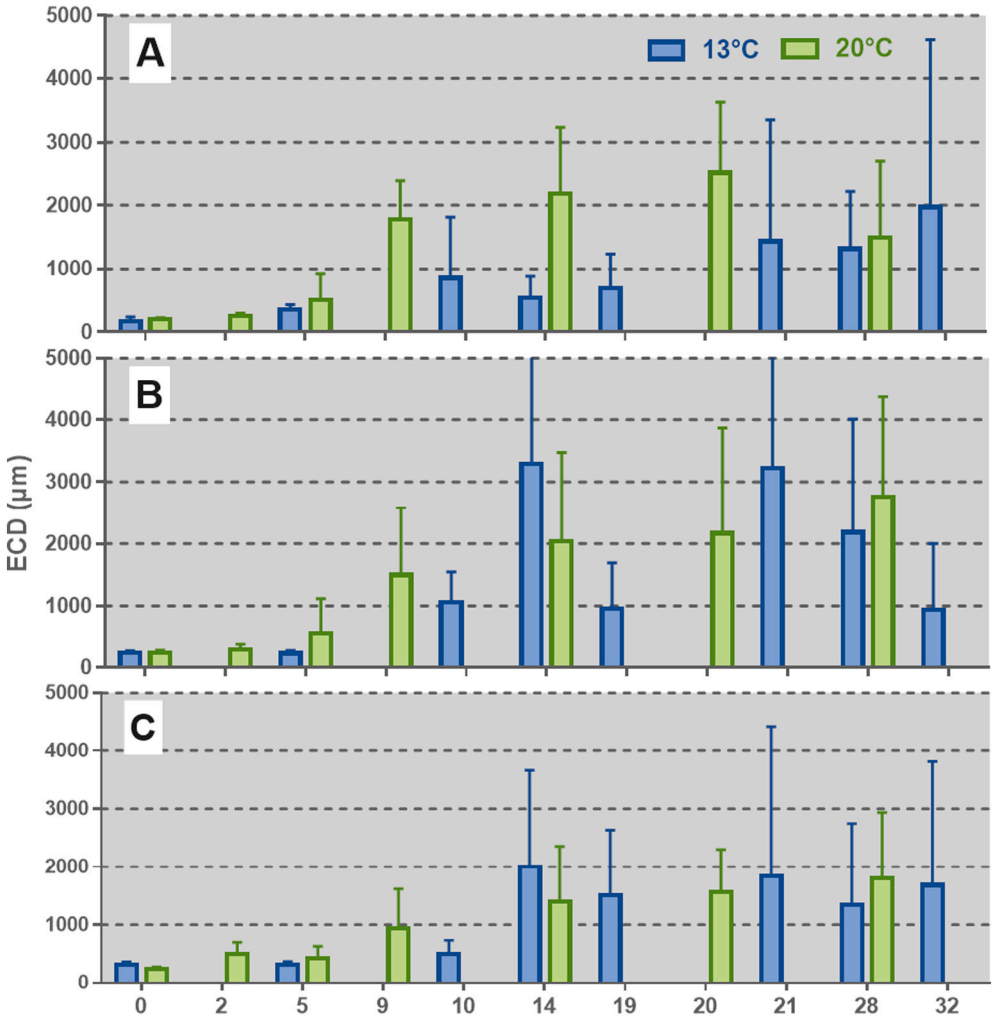

Fig. 1. Median equivalent circular diameter (ECD) of triplicate samples, determined by SilCam analyses of ORAs formed over time during incubation of 15 mg/L oil (A), oil with 10,000 cells/mL algae (B) and oil, algae and 5 ppm mineral particles (C), incubated at 13 °C or 20 °C for up to 32 or 28 days, respectively. Standard deviations are shown by error bars.

(Figs. S2 and S3), indicating that the oil droplets became incorporated into the diatom, as also previously reported (Passow et al., 2019; Wirth et al., 2018). Oil droplet concentrations were also reduced in relations to aggregation in treatments without diatoms or mineral particles (results not shown), in which aggregation has been associated with EPS-producing bacteria (Fu et al., 2014). However, no significant aggregation was measured in sterilized controls incubated at 13 °C and 20 °C (Fig. S2). As shown from the large standard deviations (Figs. 1 and S2), median aggregate sizes differed considerably between replicates. The large variations between replicates were expected, since ORA formation in the individual replicates is subject to continuous formation and disintegration processes in each sample.

While MarS formation is a physical coagulation process of marine particles, formation of ORAs may be caused by both bacterial and algal processes (Alldredge and Silver, 1988; Fu et al., 2014; Passow et al., 2012, 2019; Ziervogel et al., 2012; Wirth et al., 2018). The formation of aggregates with dispersed oil in SW without diatoms and mineral particles was assumed to be driven by bacterial processes, as previously shown in both DWH deep sea samples and laboratory studies (Bælum et al., 2012; Fu et al., 2014; Hazen et al., 2010). Spectromicroscopic studies have shown that this type of aggregates consists of proteins, carbohydrates, alkanes and oxidation products, associated with microorganisms, carbohydrates, oil, and oil degradation products (Bælum et al., 2012; Hazen et al., 2010). These processes are expected to depend on EPS-producing oil-degrading bacteria (Gutierrez et al., 2013, 2018). The importance of bacterial processes in ORA formation was confirmed in our studies by the fact that aggregates were formed in SW without diatoms and mineral particles. In addition, the lack of aggregation in sterilized controls was probably the result of inhibition of EPS production and thereby loss of stickiness. In our studies ORAs often appeared both as elongated and more compact structures. The presence of diatoms resulted in larger aggregates by time than in oil without algae, probably caused by the combined coagulation by mucus-producing bacteria and diatoms, although the aggregate sizes did not differ significantly ($P > 0.05$) in the two systems (Fig. 1).

At 20 °C, the aggregation seemed to be faster than at 13 °C. However, the presence of mineral particles together with diatoms seemed to reduce aggregate sizes compared to treatments with oil and diatoms without mineral particles. The reduced aggregate sizes in the presence of the diatoms towards the end of the experiment at 13 °C, after peak levels at 20–21 days (Fig. 1), could be the result of microbial degradation of aggregate material, resulting in fragmentation, possibly caused by release of dissolved organic carbon and microbial degradation (Goldthwait et al., 2005). In agreement with the smaller aggregates in the presence of mineral particles, it has been reported that coaggregation of algae and clay has resulted in reduced aggregate size and increased densities when compared to aggregation with algae alone, because the sticky algal surfaces may be saturated with mineral particles, reducing the stickiness and destabilizing the aggregates (Hamm, 2002).

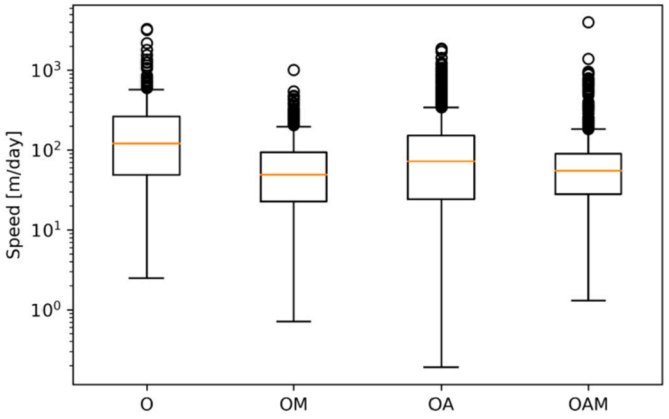

Fig. 2. Boxplots of sinking speed of ORAs formed after 8–9 days of incubation at 20 °C, with 15 mg/L oil droplets (O), oil droplets with mineral particles (OM), oil droplets with algae (OA), and oil droplets, algae and mineral particles (OAM). The data are shown for ORAs within the range of 0.2 to 1.0 mm. The boxes represent the 25th and 75th percentiles, the orange line the 50th percentile (median), the whiskers extend to 1.5 × IQR (Inter Quartile Range), while the circles are outliers beyond this range.

3.2. Aggregate sinking properties

The high densities of the aggregates with mineral particles (Engel et al., 2009; Passow and De La Rocha, 2006) were substantiated by the observations that mineral particles were necessary for the aggregates to sink at the lower temperatures (5 °C and 13 °C). At these temperatures, ORAs without mineral particles were subject to both sinking and rising behaviour, in agreement measurements from other studies (Fu et al., 2014). Faster formation of aggregates in experimental systems with mineral particles and algae have been reported due to increased collision probabilities and increase of specific weight and faster sinking velocities when lithogenic particles stick to biogenic material (Hamm, 2002). At 20 °C incubations, aggregates without mineral particles also showed sinking properties to a greater extent, as shown also in recent laboratory studies (Passow et al., 2017). Aggregate sinking velocities were determined by SilCam particle tracking analyses above the bottom of a settling column (Fig. S1) after incubation for 8–9 days, resulting in sinking speeds ranging from 50 m/day to > 200 m/day, and no significant differences in speed were determined between the treatments (Fig. 2). The large sinking velocity range was partly in agreement with data from other studies. For instance, the sinking velocities of settling ORAs collected in relation to the DWH oil spill range from 68 to 553 m (Passow et al., 2012), comparable to sinking velocities of natural MarS in the GoM (Diercks and Asper, 1997). Data on sinking rates of natural MarS from lab and field studies have been reported to range from 1 to 368 m/day (Alldredge and Silver, 1988).

ORA sinking rates have been reported to be related to aggregate size (Passow et al., 2019). However, sinking rates did not seem to be a function of aggregate sizes in our studies (Fig. S4, Supplementary information). While most oils, due to their lower densities than SW, should counteract the sinking properties of marine aggregates, experimental data of oil diatom aggregates have shown that oil may stimulate sinking. The oil may decrease the porosity of the aggregates, allowing for tighter packing of algae due to capillary bridging between algae and oil droplets, and thus increasing the ORA densities and their sinking velocities (Passow et al., 2019).

3.3. Accumulation of oil compound groups in the ORAs

As mentioned above, the aggregate sizes were determined in the incubations at 13 °C and 20 °C. In Fig. 3, the aggregate sizes, given as equivalent circular diameter (ECD), were related to accumulation and depletion of *n*-alkanes, naphthalenes, 2- to 3-ring PAHs, 4- to 6-ring PAHs, and the sum of the semivolatile organic compounds (SVOCs), quantified by GC–MS analyses and normalized against the recalcitrant oil compounds 30ab hopane (Prince et al., 1994). Fractions of the *n*-alkanes were measured in the aggregates in the presence of algae and algae + mineral particles already at day 0 in microcosms at 13 °C (7.9 ± 0.6% with algae and 21.8 ± 3.1% with algae and mineral particles), and even more at 20 °C (24.1 ± 1.6% with algae and 31.7 ± 1.9% with algae and mineral particles), as shown in Table S2a and b (Supplementary information). Since *n*-alkane attachment was considerably lower in dispersed oil without algae and mineral particles (1.9 ± 1.4% at 13 °C and 13.5 ± 0.6% at 20 °C, Table S2), oil presumably attached rapidly to diatom and mineral particle surfaces. The fractions of more water-soluble oil compounds like naphthalenes, were lower in the aggregates at the start of the experiments (≤9% at 13 °C and ≤16% at 20 °C in the presence of algae and mineral particles, and 2.2 ± 0.4% and 6.4 ± 0.2% in oil alone at 13 °C and 20 °C, respectively; Table S2). After close to 3 weeks of incubation at 13 °C, when the aggregate sizes peaked, the maximum accumulations of all SVOC compounds reached 83.9 ± 1.5% and 89.0 ± 3.9% in the aggregates with oil + algae and oil + algae + mineral particles, while the accumulated fractions were lower (60.9 ± 0.11.8%) in aggregates with oil alone (Table S2a). Recent studies with dispersed oil and phytoplankton-based ORAs showed that while alkanes and high-molecular weight PAHs were rapidly integrated in ORAs as part of the oil droplets, more water-soluble naphthalenes and low-molecular weight PAHs, were dissolved from the droplets, and then accumulated in ORAs sorption processes (Wirth et al., 2018). This may explain the relatively high 0-day n-alkane fractions in the ORAs, while the corresponding fractions of water-soluble naphthalenes were lower in the ORAs, but increased by time.

Comparison of oil compound group accumulations at 13 °C and 20 °C showed significantly lower accumulation in oil alone than in oil + algae or oil + algae-mineral particles ($P < 0.05$; two-tailed *t*-test) after 3 weeks of incubation. The higher relative concentrations of oil compound groups in the aggregates from incubations with the diatoms present, compared to oil alone, were determined by average factors of 2.0 at 13 °C and 1.6 at 20 °C after 3 weeks. Likewise, the aggregate accumulations of oil compounds were also faster in the presence of algae, by a factor of 1.3 after 5 days at 13 °C and 1.8 at 20 °C (Table S3, Supplementary information), i.e. faster ORA uptake of oil compound groups at 20 °C than 13 °C. These data showed that the presence of diatoms in the aggregates contributed to the accumulation of the oil compound groups. The high fractions of oil compounds in the aggregates by time (Fig. 3 and Table S2) could be the result of a combination of oil droplet integration and compound sorption and of faster biodegradation in the SW than in the aggregate fractions.

Experiments performed in cold SW at 5 °C with dispersed oil alone, or oil with algae, also showed accumulations of oil compound groups (*n*-alkanes, naphthalenes, 2- to 3-ring PAHs, 4- to-6-ring PAHs, SVOC) in the aggregates. These compounds were mainly measured in the water-phases early in the incubation period, with ≤2% in aggregates at day 0, and ≤ 8% at 5 days (Table S2c). Thereafter, the oil compounds were largely measured in the aggregates, with a maximum of 86.2 ± 3.4% of the 2- to 3-ring PAHs in the aggregates at day 64 (Table S2c). Also in these incubations, the relative accumulations of oil compounds in the aggregate fractions were faster in incubations with algae than with oil alone, although accumulation of oil compound groups were not significantly different in oil alone and oil-algae ($P > 0.05$; two-tailed t-test). After 21 days of incubations, the relative distributions of oil compounds were higher by an average factor of 1.6 in aggregates with algae than without algae, while this factor was reduced to 1.1 after 64 days (Table S3c).

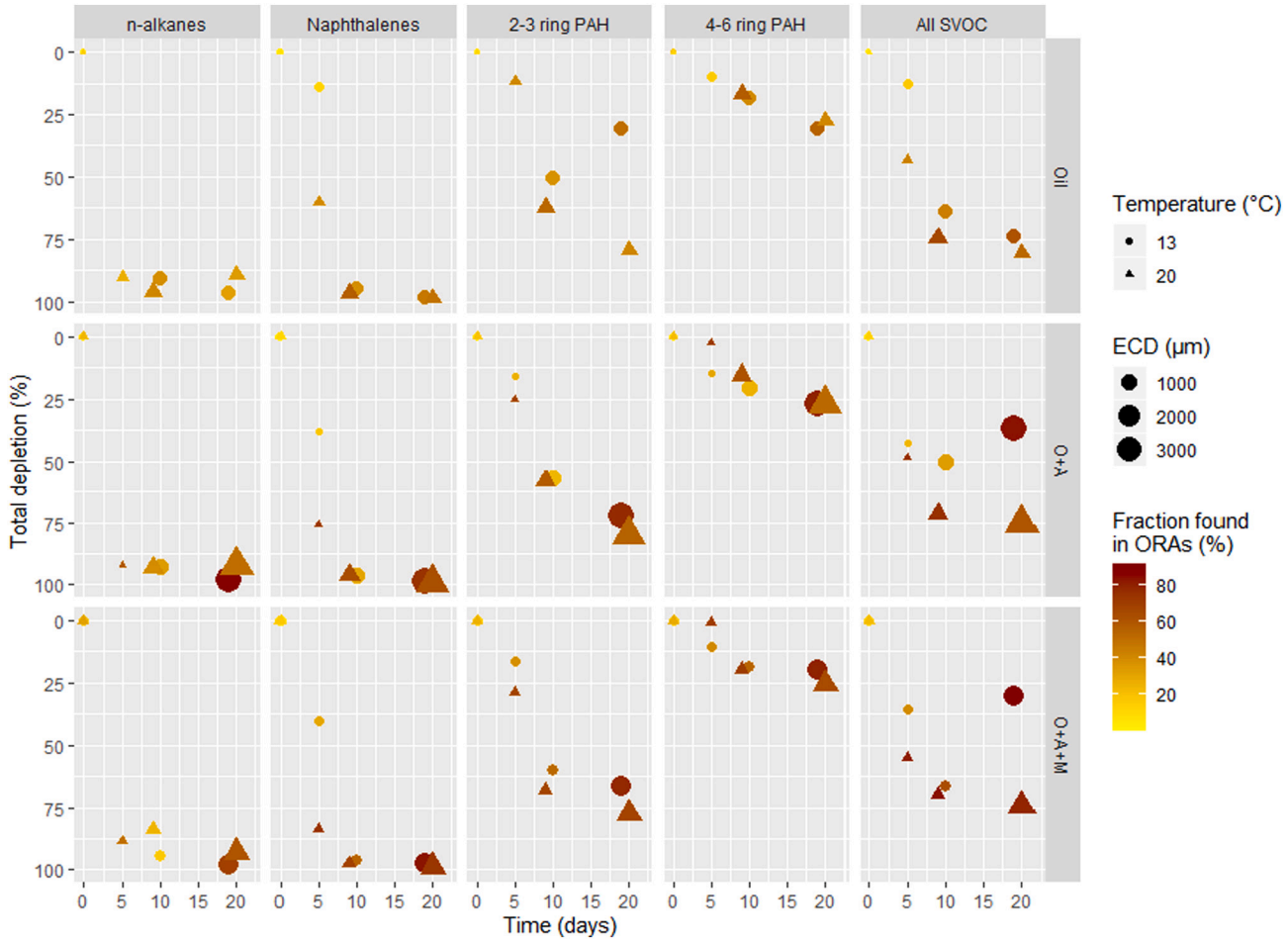

Fig. 3. The total depletion (sum of WP + ORA, normalized against 30ab hopane) of *n*-alkanes, naphthalenes, 2–3 ring PAH, 4–6 ring PAH and all SVOC compounds in the microcosm experiment incubated at 13 °C (●) and 20 °C (▲) over time. The size of the symbols corresponds to the size of ORAs (ECD in µm), while the colour gradient indicates the fraction (%) found in ORAs, with dark red representing the highest fraction. Treatments contained 15 mg/L oil droplets (O), oil droplets and the algae *S. pseudocostatum* (O + A), and oil droplets, the algae *S. pseudocostatum* and mineral particles (O + A + M). (For interpretation of the references to colour in this figure legend, the reader is referred to the web version of this article.)

3.4. Biotransformation of oil compound groups

Since the experiments were performed in closed test systems without headspace and air-bubbles, evaporation was avoided, and we assumed that the depletion of oil compounds was the result mainly of biotransformation. This was also confirmed by comparison of depletion in treatments with normal and sterilized SW (Fig. S5, Supplementary information). Quantification of hopane-normalized oil compound groups showed that biotransformation of *n*-alkanes and PAH groups was mainly comparable in all treatments at each incubation temperature at the end of the incubation periods, as shown in Fig. 3, and in Fig. S6 and Table S4 (Supplementary information), although higher fractions of the oil compounds were present in the aggregates with algae and algae + mineral particles than in incubations with oil alone (Table S2). For instance, the depletion of the oil droplet-associated n-alkanes at the end of the experiments varied between 97.0 ± 0.2% and 98.2 ± 0.1% at 13 °C, between 89.3 ± 0.4% and 92.9 ± 0.6% at 20°, and between 62.8 ± 10.7% and 72.4 ± 9.5% at 5 °C (Table S4). For the more water-soluble naphthalenes, the corresponding data were 96.1 ± 0.1% to 98.3 ± 0.2% at 13 °C, 98.7 ± 0.1% to 98.9 ± 0.1% at 20 °C, and 92.1 ± 1.8% to 92.3 ± 2.6% at 5 °C (Table S4). The depletion of *n*-alkanes was faster than the depletion of 2- to 6-ring PAHs (also including naphthalenes), mainly caused by the slower depletion of the 2- to 3-ring and 4- to 6-ring PAHs at all temperatures (Figs. 3, S6, Table S4), and with oil residues ending up in large ORAs at the end of the experiments, particularly in the oil + algae treatments (Fig. 3). We anticipate that while *n*-alkanes were mainly biodegraded in the ORAs as part of oil droplets directly integrated in the aggregates, the PAHs, depending on their water-solubilities, were subject to a combined dissolution and subsequent sorption to the aggregates, and with biodegradation of these compounds both in seawater and the ORAs (Wirth et al., 2018).

Biotransformation of the oil compound groups was mainly similar between incubations at 13 °C and 20 °C for all treatments (oil alone, oil + algae, oil + algae + mineral particles), as shown in Fig. 3. Only SVOC (sum of GC–MS analytes) showed poorer depletion at 13 °C than at 20 °C, following a typical temperature-related biodegradation trend, and only in treatments with diatoms. However, at 5 °C, depletion was slower than at the higher temperatures (Fig. S6, Table S4). The similarities between compound group biotransformation at 13 °C and 20 °C were further substantiated by determination of rate coefficients and half-lives for *n*-alkanes and 2- to 6-ring PAHs (naphthalenes included) from first-order rate calculations by non-linear regression analyses. Only n-alkane transformation at 13 °C showed an initial lag-period before depletion. The *n*-alkanes and 2- to 6-ring PAHs (sums of compound groups in water-phase samples (WPs) and ORAs) showed biotransformation half-lives of 5–6 days at 13 °C, 1–3 days at 20 °C, and 26–44 days at 5 °C (Fig. 4). While biotransformation of *n*-alkanes and PAHs in incubations with algae at 13 °C were mainly comparable or faster than results from previous studies in our lab, using chemically

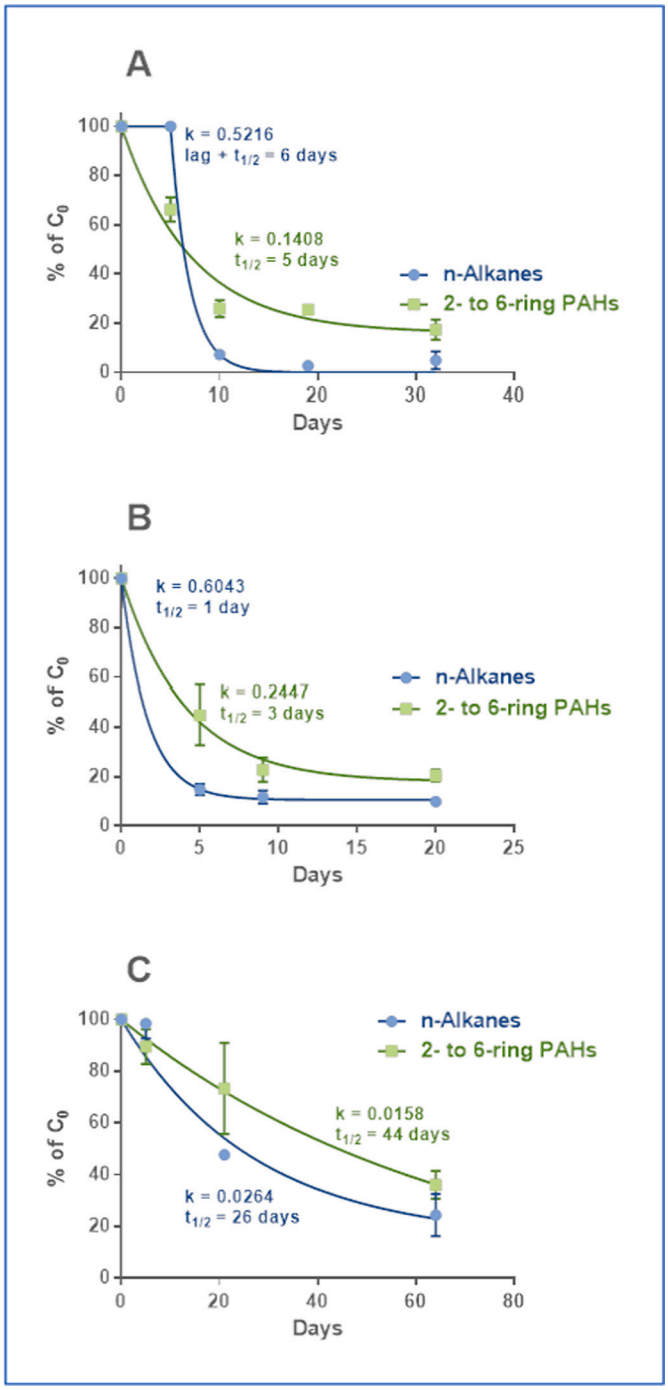

Fig. 4. Non-linear regression analyses of *n*-alkanes and 2- to 6-ring PAH biotransformation in treatments with oil + algae at 13 °C (A), 20 °C (B) and 5 °C (C). First-order rate coefficients (k) and half-lives ($t_{1/2}$) are shown. The calculations are based on the sums of the concentrations in water sampless and ORAs, after normalization against 30ab hopane (A and B), or the sum of pristane and phytane (C).

dispersed oil and the experimental systems (Brakstad et al., 2018a), biotransformation at 5 °C was slower than in previous carousel experiments (Brakstad et al., 2018b; Ribicic et al., 2018b). Also results for *n*-alkanes and PAHs at 20 °C compared well to previous laboratory data with crude oil dispersed with Corexit 9500 (Venosa and Holder, 2007). The results from these experiments therefore indicated that the aggregation caused by diatoms/mineral particles did not affect biodegradation significantly, when compared to data from studies in SW without these particles. This is important information, showing that biodegradation processes will not be significantly affected by aggregation processes. Biodegradation will therefore continue after aggregation and ORA formation. During the DWH oil spill, oil weathering processes, including dissolution and biodegradation, continued also after ORA sedimentation, leaving mainly highly weathered oil residues on the seabed when sediment cores were samples 1 to 4 years after the spill (Bagby et al., 2017; Stout and Payne, 2016; Yergeau et al., 2015).

Considerable biodegradation in the test systems was also confirmed by the consumption of dissolved oxygen in the treatments, resulting in average DO consumptions in oil-containing samples of 5.1 ± 1.3 mg at 13 °C, 5.2 ± 1.4 mg at 20 °C, and 6.6 ± 0.8 mg at 5 °C (Fig. S7, Supplementary information). The DO reductions were significantly higher in treatments with algae when compared to treatments with oil droplets ($P < 0.05$; paired *t*-tests). Since oil biotransformation data did not differ much between the treatments with and without algae, the higher DO consumptions in treatments with algae were probably associated with heterotrophic degradation of algal material (Piontek et al., 2009).

3.5. Microbial community structures in aggregates and SW phases

The microbial compositions in aggregates and corresponding water phases were investigated by 16S rRNA gene amplicon sequencing of separated ORA and WP samples from incubations at the three temperatures. Relative bacterial abundances (genus level) in samples from incubations with diatoms (oil + algae and oil + algae + mineral particles) were greatly influenced by microbes associated with the algae, as also previously reported (Netzer et al., 2018). In the incubations at 13 °C and 20 °C, including *S. pseudocostatum* as algal species, high abundances of *Owenweeksia* were observed, particularly in aggregate samples from days 0 and 5. While *Owenweeksia* remained abundant in the aggregates for at least 9–10 days, the genus became rapidly outcompeted by other groups in the water phases (Fig. S9a and b, Supplementary information). In incubations at 5 °C (including *F. cylindrus* as algal species), correspondingly high abundances of *Nonlabens* were observed throughout the whole experimental period (Fig. S9c), as also previously reported (Netzer et al., 2018). The persistence of *Nonlabens* throughout the 2-months experimental period at 5 °C, indicated potentials for utilization of hydrocarbons as energy source (Netzer et al., 2018). Hydrocarbon degraders have previously been reported to co-occur with phytoplankton (Gutierrez et al., 2014; Kamalanathan et al., 2019). Studies with oil-contaminated aggregates of faeces from the copepod *Calanus finmarchicus* also revealed that typical heterotrophic bacteria associated with the normal copepod faeces were involved in oil biodegradation (Størdal et al., 2015). Several of the identified genera which became abundant during the biodegradation periods are associated with oil biodegradation, including *Alcanivorax* (13 °C and 20 °C), *Alteromonas* (13 °C and 20 °C), *Colwellia* (13 °C, 20 °C and 5 °C), *Cycloclasticus* (13 °C, 20 °C and 5 °C), *Ulvibacter* (13 °C), *Marinobacter* (13 °C and 5 °C), *Porticoccus* (20 °C), *Sulfitobacter* (13 °C and 20 °C), *Oleibacter* (13 °C and 20 °C), *Oleispira* (13 °C and 5 °C), and *Thalassolituus* (13 °C). Several of these genera (*Alcanivorax*, *Marinobacter*, *Oleibacter*, *Oleispira*, *Cycloclasticus,* and *Thalassolituus*) are considered to include typical obligate hydrocarbonoclastic species (Yakimov et al., 2007). While genera like *Alcanivorax*, *Oleibacter* and *Oleispira* are associated with alkane degradation (Yakimov et al., 2007), *Cycloclasticus* is highly associated with degradation of aromatic hydrocarbons (Dyksterhouse et al., 1995; Geiselbrecht et al., 1998; Messina et al., 2016).

More detailed stimulations of specific microbial genera are shown in heat maps (Fig. 5), specifically showing similarities and differences between relative abundances in aggregates and water phases and between the different treatments. The diatom-related genera were typically associated only with aggregates at 13° and 20 °C (*Owenweeksia*), but were also abundant in SW a 5 °C (*Nonlabens*), indicating higher associations with algal cells of *Owenweeksia* than *Nonlabens*. However,

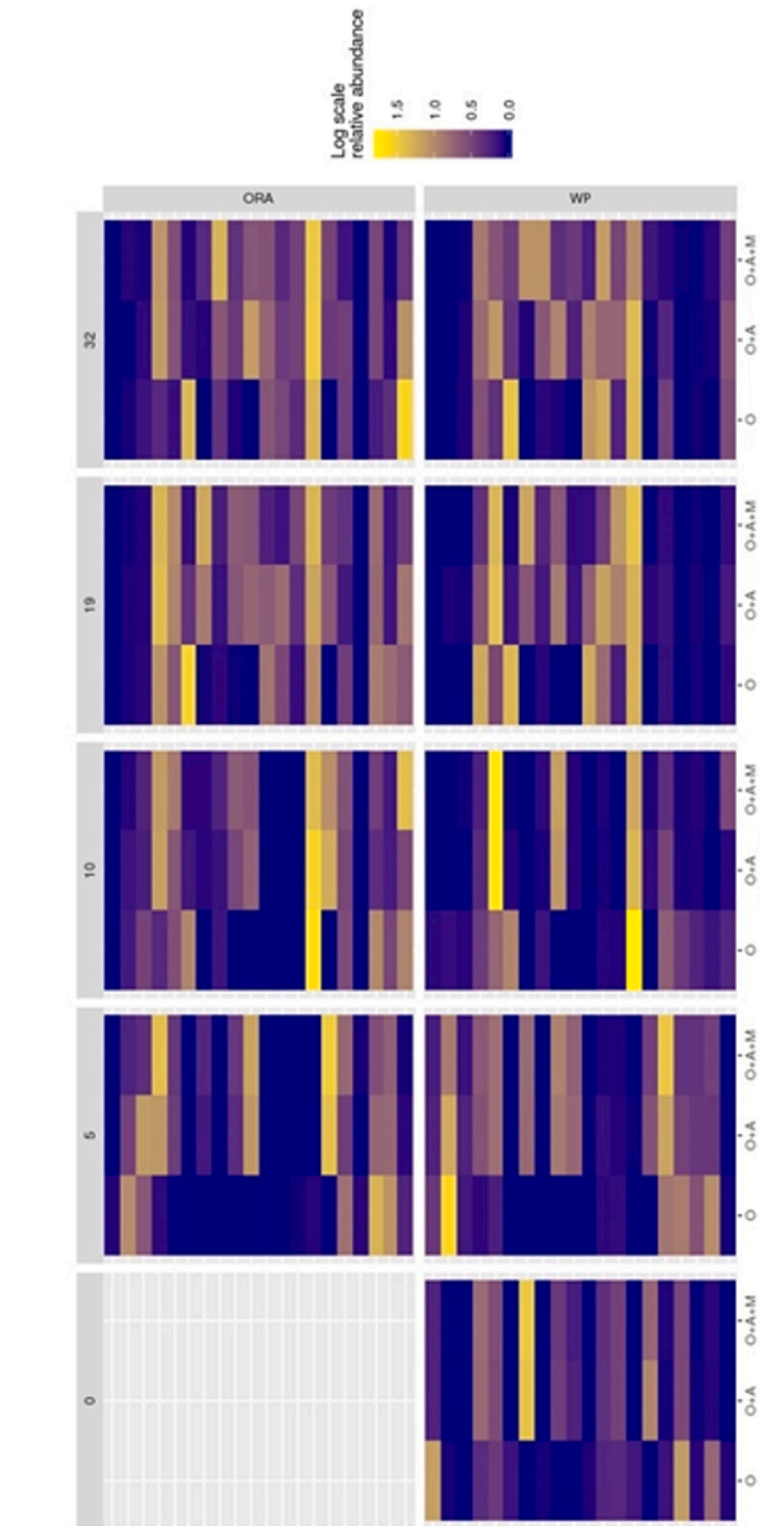

Fig. 5. Heatmap showing of the relative abundance of bacteria (at a Family/Genus level) found over time in the ORAs and water phases (WPs) of the microcosm experiments incubated at 13 °C (A), 20 °C (B), and 5 °C (C). Treatments at 13 °C and 20 °C contained oil droplets (O), oil droplets and the algae *S. pseudocostatum* (O + A), and oil droplets, the algae *S. pseudocostatum* and mineral particles (O + A + M). Treatments at 5 °C contained oil droplets (Oil), oil droplets and the algae *F. cylindrus* (Oil + Algae), or the algae *F. cylindrus* without oil (Algae).

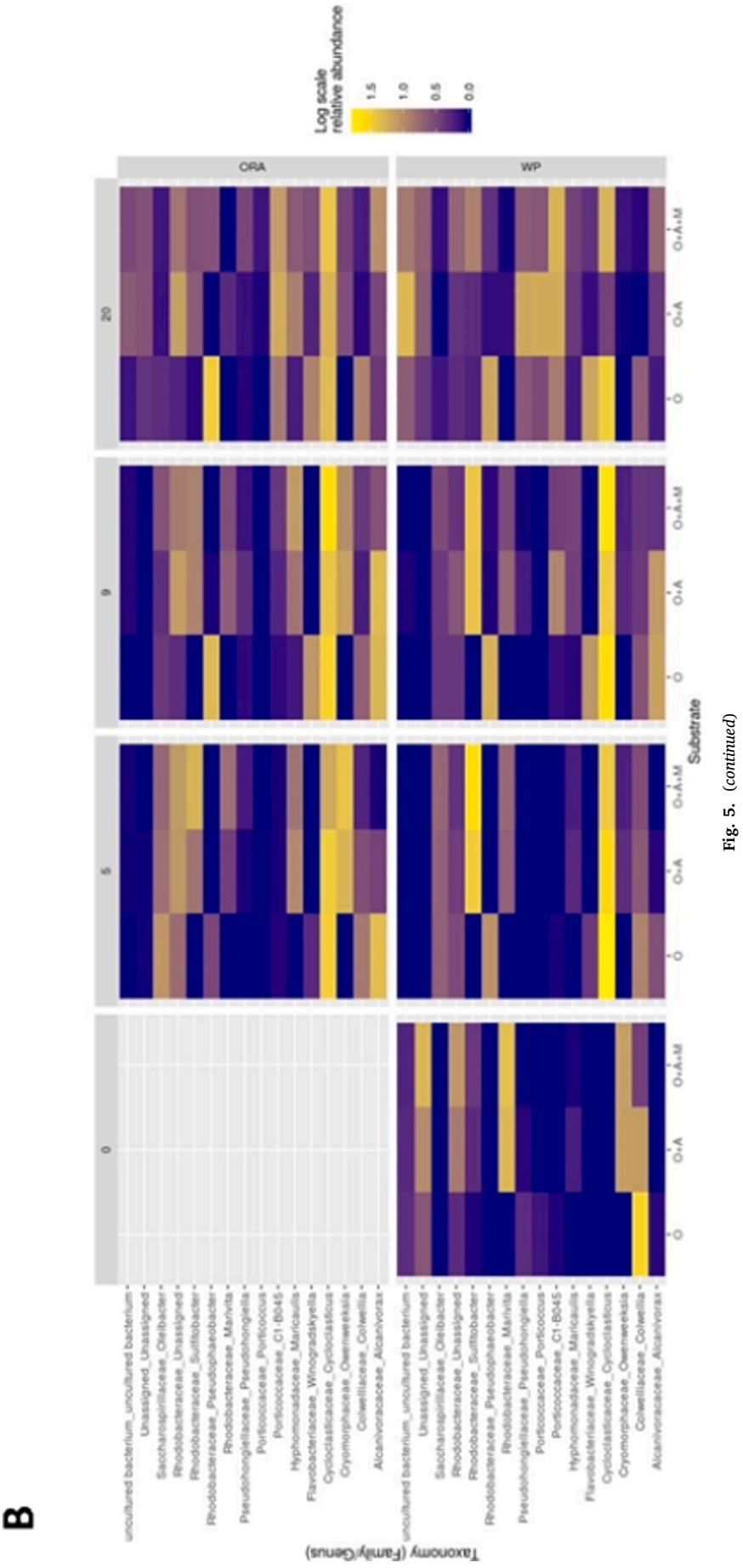

Fig. 5. (*continued*)

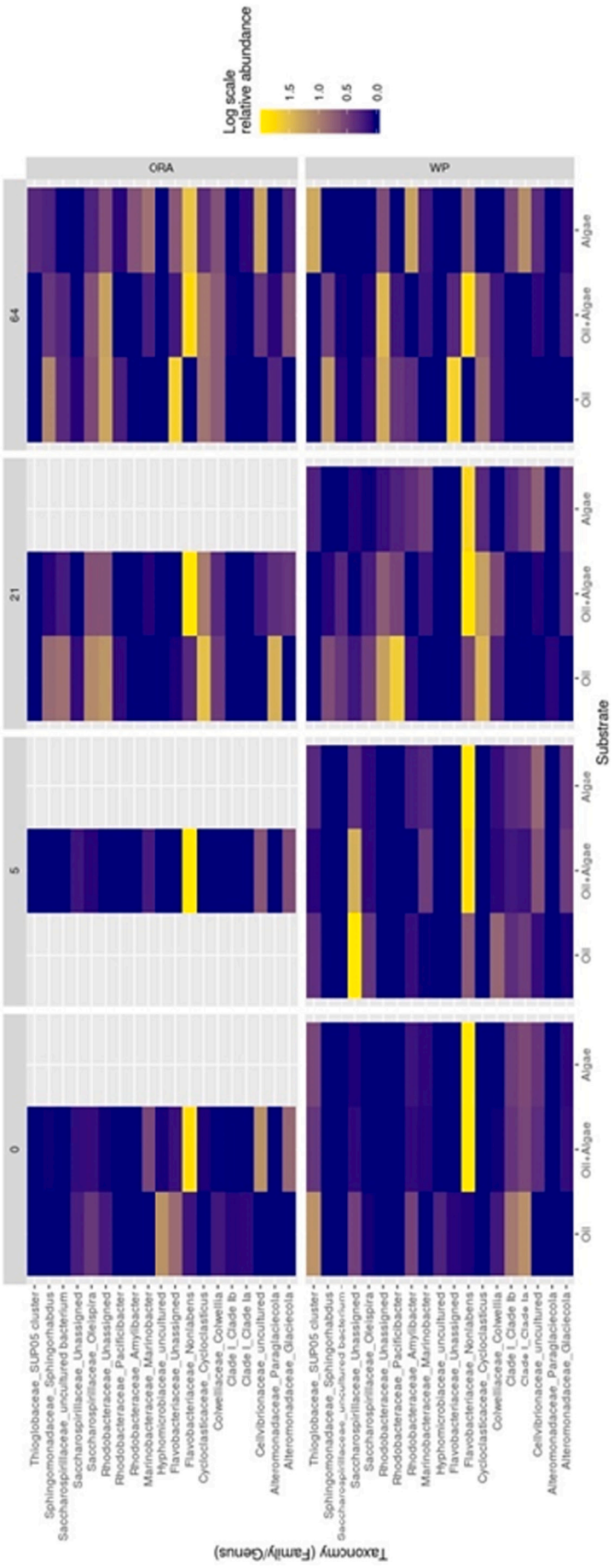

Fig. 5. (*continued*)

Nonlabens may also be related to the possible involvement in oil biodegradation processes (Netzer et al., 2018). Alkane-degraders like *Oleispira* (5 °C), *Oleibacter* (13 °C and 20 °C) and *Alcanivorax* (13 °C and 20 °C) typically appeared with higher relative abundances in aggregates than in water phases in incubations both with oil alone and oil + algae (+mineral particles). The abundances of *Oleispira* at 5 °C and *Oleibacter* at 13 °C are in agreement with the general temperature preferences of species in two *Saccharospirillaceae* genera (Teramoto et al., 2011; Yakimov et al., 2003), while *Alcanivorax* is considered to be mesophilic (Cappello and Yakimov, 2010). In contrast to the alkane-degraders, the aromatic hydrocarbon degrader *Cycloclasticus* became abundant in both aggregate and water phases in all treatments (oil alone, oil + algae, oil + algae + mineral particles) at all temperatures, although faster in water than aggregate phases at 5 °C. These differences between the alkane- and aromatic hydrocarbon degraders probably reflect the solubility properties of the hydrocarbon groups, in which alkanes are associated with oil droplets directly integrated in the aggregates, while the most abundant aromatic hydrocarbons were dissolved and later

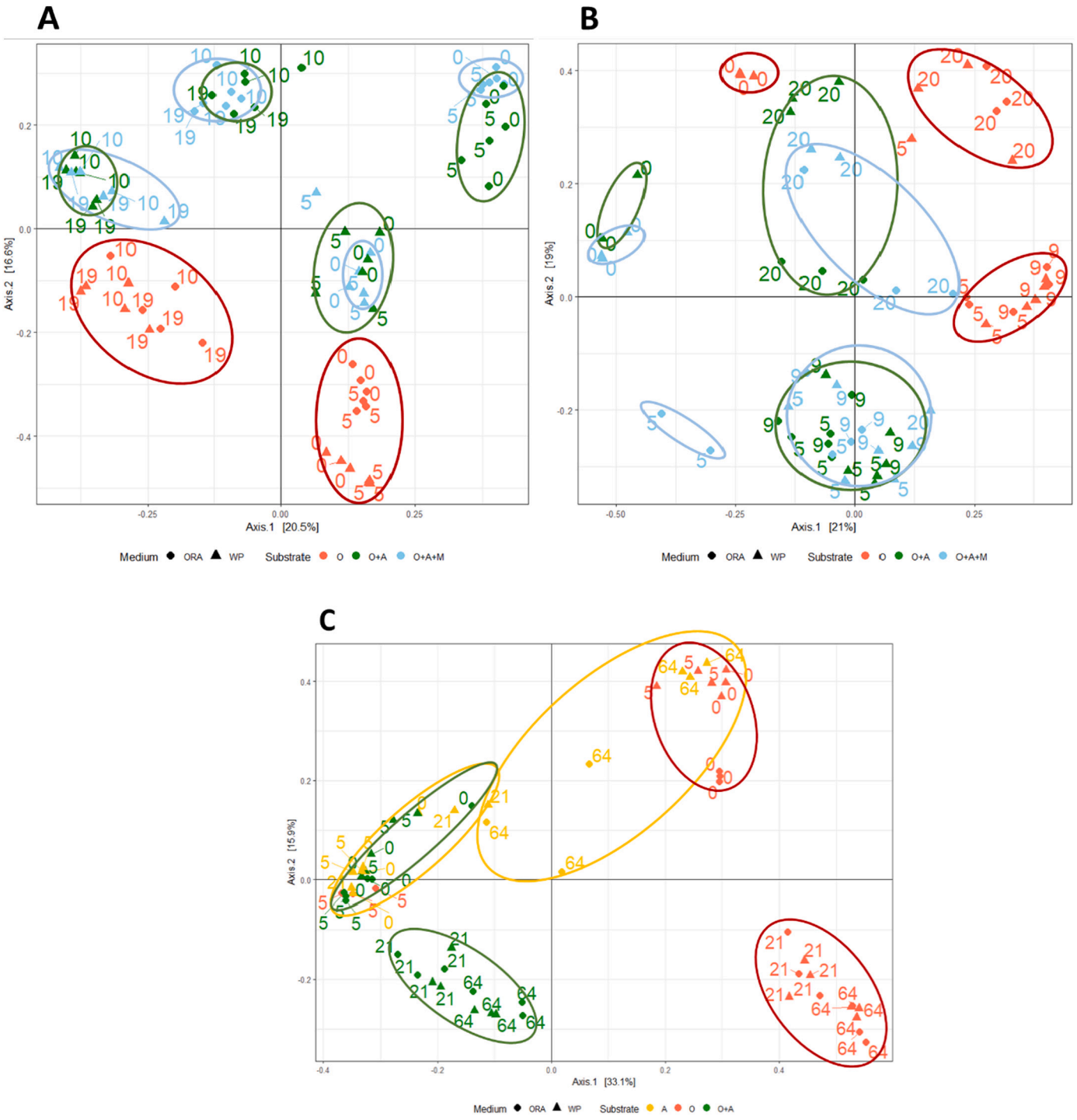

Fig. 6. Beta diversity measured by Bray-Curtis dissimilarity of samples from microcosms incubated at 13 °C (A), 20 °C (B) and 5 °C (C), including sampling date, a calculated trajectory over time, and clustering (circles). Treatments contained: A) and B) the algae *S. pseudocostatum* alone (Algae), 15 mg/L oil droplets (Oil), oil droplets and the algae *S. pseudocostatum* (Oil + Algae), or oil droplets, algae and mineral particles (O + A + M); C) 30 mg/L oil droplets (O), or oil droplets and the algae *F. cylindrus* (Oil + Algae).

sorbed to the aggregates (Wirth et al., 2018). The quantitatively predominant aromatic hydrocarbons, like naphthalenes and low-molecular PAHs, will therefore distribute between the aggregates and water. Some bacteria associated with oil biodegradation showed higher abundances early in the degradation periods in aggregates and water samples with oil + algae/mineral particles, than with oil alone, e.g. *Sulfitobacter* and other *Rhodobacteraceae* (13 °C and 20 °C). These groups may have been involved in the faster degradation of oil compounds in incubations with algae/mineral particles than in oil alone, particularly of naphthalenes and 2- to 6-ring PAHs (Table S3a and b).

The microbial diversities, measured by the Shannon indexes, were found to be similar in the ORAs and the corresponding water samples at all temperatures (Fig. S10, Supplementary information), although the microbial diversity was slightly higher at 13 °C and 20 °C than at 5 °C (Fig. S10). The onset of hydrocarbon biodegradation was typically accompanied by a loss in biodiversity, which was observed in both phases at all three temperatures. This was expected, since only a limited number of bacteria are able to utilize hydrocarbons as carbon source (Yakimov et al., 2007). Interestingly, at 13 °C the aggregate fraction showed a drop in diversity at day 5, while in the water phase this loss in diversity occurred later at day 9 (Fig. S10a).

The beta diversity was calculated with the Bray-Curtis dissimilarity index and showed a distinct clustering of the oil treatments containing algae (O + A, O + A + M), compared to oil dispersion without algae (O), shown in Fig. 6, both with *S. pseudocostatum* at 13 °C and 20 °C and *F. cylindrus* at 5 °C. Less separation was observed between samples with oil + algae and oil + algae + mineral particles, inferring that the diatoms rather than the mineral particles were the drivers for the differences in bacterial communities. In addition, the differences between microbial communities in aggregate and water fractions were small to negligible, with the exception of the 64-days samples from incubations at 5 °C, where aggregate and water samples clustered separately for diatoms without oil (A) (Fig. 6c). We have recently shown by PCA plots that both oil chemistry and microbial community successions followed trajectory pathways during oil biodegradation processes (Ribicic et al., 2018a). Particularly in incubations at 13 °C, clusters followed pathways along Axis1, between days 5 and 10 at 13 °C (Fig. 6a), in which the main biodegradation of *n*-alkanes, naphthalenes, 2- to 3-ring PAHs and SVOC took place (Fig. 3 and Table S4a). In 5 °C incubations, the clusters largely followed pathways along Axis2 day 5 to 21 (Fig. 6c), in agreement with biodegradation of *n*-alkanes and naphthalenes, while the major degradation of 2- to 6-ring PAHs and SVOC between days 21 and 64 did not result in any pathways or cluster separations (Fig. 3 and Table S4c). Incubations with algae alone (no oil) also followed a pathway, although in a separate direction along the Axis1 compared to the oil incubations (Fig. 6c), reflecting the importance of the oil for the microbial community successions in these incubations. In the 20 °C incubations, more complex clustering pathways were observed. Incubations with oil alone followed pathways along the Axis1 as in the 13° incubations, from days 0 to day 5, in agreement with the major biodegradation period of *n*-alkanes and naphthalenes (Fig. 6b), while the main 2- to 3-ring PAH and VOC degradation period between days 5 and 9 was not reflected in any pathways (Fig. 3 and Table S4b). However, incubations with oil + algae and oil + algae + mineral particles followed changes along the Axis2 to a greater extent, without any obvious relations to oil biodegradation patterns (Fig. 6b).

4. Conclusions

Incubations of chemically dispersed oil in natural non-amended SW at different temperatures were performed in associations with diatoms and mineral particles, which are associated with the formation of MarS. Concentrations of dispersed oil were typically reduced at the same time as aggregation of macroscopic ORA particles were observed during the incubations. In our studies both the presence of algae/mineral particles and SW temperatures were important for the formation and fate of crude oil. The presence of the diatoms used in this tudy seemed to stimulate to faster formation of aggregates, incorporating large fractions of hydrocarbons. The algae and mineral particles did not seem to affect biotransformation when compared to oil alone. In the incubations without algae, aggregates were also observed, probably produced by EPS-producing bacteria. Microbial community analyses showed that the aggregates became inhabited by typical oil-degrading bacteria, and that the presence of oil was important for the microbial community successions in the incubations. The community results also indicated that bacteria initially associated with algal species could contribute to oil compound biodegradation.

The different SW temperatures also affected both aggregate formation and fate of the oil. The aggregation seemed to be faster in relation to SW temperature. Higher fractions of measured oil compounds accumulated in aggregates containing algae/mineral particles than in aggregates in SW alone at all three temperatures, and both *n*-alkane and PAH biotransformation were faster at the two higher temperatures than at 5 °C. The biotransformation of *n*-alkanes and PAH was comparable between all treatments at the same temperatures. Finally, SW temperature seemed to be important for the aggregate sinking properties, since high temperature (20 °C) was required for particle sinking in the absence of mineral particles, and at this temperature aggregates formed in SW without algae and mineral particles also showed sinking properties.

The use of chemical dispersants, with the formation of small-droplet oil dispersion, therefore resulted in the aggregation of considerable amounts of oil compounds in SW at different temperatures, but without any particular influence on oil biodegradation, as the aggregates became inhabited by microbial communities involved in oil compound biodegradation. However, our results indicated that it was only at high SW temperatures that aggregates without mineral particles resulted in predominantly sinking properties, and with possible ORA sedimentation. At lower SW temperatures, mineral particles were required for massive aggregate sinking, while ORAs without mineral particles showed both rising and sinking behaviour. This may imply that sinking of ORAs in temperate and cold SW may be a process associated with coastal rather than oceanic SW, although we still consider these processes to be debatable. In relation to chemically dispersed oil, we further lack information on attachment and sorption processes of rapidly diluted oil dispersions to marine particles and the possible fate of the oil if these particles aggregate after oil attachment.

CRediT authorship contribution statement

Ingrid A. Henry: Conceptualization, Data curation, Formal analysis, Investigation, Methodology, Resources, Software, Validation, Visualization, Writing - original draft.**Roman Netzer:**Conceptualization, Data curation, Formal analysis, Methodology, Software, Supervision, Validation.**Emlyn J. Davies:**Conceptualization, Data curation, Formal analysis, Investigation, Methodology, Software, Validation, Visualization.**Odd Gunnar Brakstad:**Conceptualization, Data curation, Formal analysis, Funding acquisition, Investigation, Project administration, Resources, Supervision, Validation, Writing - original draft.

Declaration of competing interest

The authors declare that they have no known competing financial interests or personal relationships that could have appeared to influence the work reported in this paper.

Acknowledgments

The research described in this paper was funded by the Research

Council of Norway through the Petromaks2 program (contract #267767/E30), and the oil companies Equinor ASA and TOTAL E&P Norge AS. We would like to thank Marianne Unaas Rønsberg, Inger K. Almås, Marianne Aas, Lisbet Støen and Lisbet Sørensen for chemical analyses and experimental assistance, and Deni Ricibic for providing scripts and guidance through the bioinformatics analysis. Bioinformatics support was also provided through by the BMBF-funded project "Bielefeld-Gießen Center for Microbial Bioinformatics - BiGi (Grant Number 031A533)" within the German Network for Bioinformatics Infrastructure (de.NBI) is gratefully acknowledged.

Appendix A. Supplementary data

Supplementary data to this article can be found online at https://doi.org/10.1016/j.marpolbul.2020.111483.

References

Alldredge, A.L., Silver, M.W., 1988. Characteristics, dynamics and significance of marine snow. Prog. Oceanogr. 20, 41–82.
Aslam, S.N., Cresswell-Maynard, T., Thomas, D.N., Underwood, G.J., 2012. Production and characterization of the intra-and extracellular carbohydrates and polymeric substances (EPS) of three sea-ice diatom species, and evidence for a cryoprotective role for EPS. J. Phycol. 48, 1494–1509.
Atlas, R.M., Bartha, R., 1992. Hydrocarbon Biodegradation and Oil Spill Bioremediation. In: Adv. Microb. Ecol. Springer, pp. 287–338.
Bælum, J., Borglin, S., Chakraborty, R., Fortney, J.L., Lamendella, R., Mason, O.U., Auer, M., Zemla, M., Bill, M., Conrad, M.E., 2012. Deep-sea bacteria enriched by oil and dispersant from the Deepwater Horizon spill. Environ. Microbiol. 14, 2405–2416.
Bagby, S.C., Reddy, C.M., Aeppli, C., Fisher, G.B., Valentine, D.L., 2017. Persistence and biodegradation of oil at the ocean floor following Deepwater Horizon. PNAS 114, E9–E18.
Bhaskar, P., Bhosle, N.B., 2005. Microbial extracellular polymeric substances in marine biogeochemical processes. Curr. Sci. 88, 45–53.
Bokulich, N.A., Kaehler, B.D., Rideout, J.R., Dillon, M., Bolyen, E., Knight, R., et al., 2018. Optimizing taxonomic classification of marker-gene amplicon sequences with QIIME 2's q2-feature-classifier plugin. Microbiome 6, 90.
Bolyen, E., Rideout, J.R., Dillon, M.R., Bokulich, N.A., Abnet, C.C., Al-Ghalith, G.A., ... Bai, Y., 2019. Reproducible, interactive, scalable and extensible microbiome data science using QIIME 2. Nature Biotechnol. 37, 852–857.
Brakstad, O.G., Daling, P.S., Faksness, L.-G., Almås, I.K., Vang, S.-H., Syslak, L., Leirvik, F., 2014. Depletion and biodegradation of hydrocarbons in dispersions and emulsions of the Macondo 252 oil generated in an oil-on-seawater mesocosm flume basin. Mar. Pollut. Bull. 84, 125–134.
Brakstad, O.G., Nordtug, T., Throne-Holst, M., 2015. Biodegradation of dispersed Macondo oil in seawater at low temperature and different oil droplet sizes. Mar. Pollut. Bull. 93, 144–152.
Brakstad, O.G., Farooq, U., Ribicic, D., Netzer, R., 2018a. Dispersibility and biotransformation of oils with different properties in seawater. Chemosphere 191, 44–53.
Brakstad, O.G., Ribicic, D., Winkler, A., Netzer, R., 2018b. Biodegradation of dispersed oil in seawater is not inhibited by a commercial oil spill dispersant. Mar. Pollut. Bull. 129, 555–561.
Brakstad, O.G., Altin, D., Davies, E.J., Aas, M., Nordtug, T., 2020. Interaction between microalgae, marine snow and anionic polyacrylamide APAM at marine conditions. Sci. Tot. Environ. 705, 135950.
Callahan, B.J., McMurdie, P.J., Rosen, M.J., Han, A.W., Johnson, A.J.A., Holmes, S.P., 2016. DADA2: high-resolution sample inference from Illumina amplicon data. Nature Meth 13, 581.
Cappello, S., Yakimov, M., 2010. Alcanivorax. In: Timmis, K.N. (Ed.), Handbook of Hydrocarbon and Lipid Microbiology. Springer Verlag, Berlin, pp. 1737–1748 2010.
Chanton, J., Zhao, T., Rosenheim, B.E., Joye, S., Bosman, S., Brunner, C., Yeager, K.M., Diercks, A.R., Hollander, D., 2014. Using natural abundance radiocarbon to trace the flux of petrocarbon to the seafloor following the Deepwater Horizon oil spill. Environ. Sci. Technol. 49, 847–854.
Davies, E.J., Brandvik, P.J., Leirvik, F., Nepstad, R., 2017. The use of wide-band transmittance imaging to size and classify suspended particulate matter in seawater. Mar. Pollut. Bull. 115, 105–114.
De La Rocha, C.L., Passow, U., 2007. Factors influencing the sinking of POC and the efficiency of the biological carbon pump. Deep Sea Research Part II: Topical Studies Oceanogr 54, 639–658.
Diercks, A.R., Asper, V.L., 1997. *In site* settling speeds of marine snow aggregates below the mixed layer: Black Sea and Gulf of Mexico. Deep-Sea Res. I 44, 385–398.
Dyksterhouse, S.E., Gray, J.P., Herwig, R.P., Lara, J.C., Staley, J.T., 1995. *Cycloclasticus pugetii* gen. nov., sp. nov., an aromatic hydrocarbon-degrading bacterium from marine sediments. International Journal of Syst. Evolut. Microbiol. 45, 116–123.
Engel, A., 2000. The role of transparent exopolymer particles (TEP) in the increase in apparent particle stickiness (α) during the decline of a diatom bloom. J. Plankton Res. 22, 485–497.
Engel, A., Abramson, L., Szlosek, J., Liu, Z., Stewart, G., Hirschberg, D., Lee, C., 2009. Investigating the effect of ballasting by CaCO3 in *Emiliania huxleyi*, II: decomposition of particulate organic matter. Deep Sea Research Part II: Topical Studies in Oceanogr 56, 1408–1419.
Fu, J., Gong, Y., Zhao, X., O'Reilly, S.E., Zhao, D., 2014. Effects of oil and dispersant on formation of marine oil snow and transport of oil hydrocarbons. Environ. Sci. Technol. 48, 14392–14399.
Geiselbrecht, A.D., Hedlund, B.P., Tichi, M.A., Staley, J.T., 1998. Isolation of marine polycyclic aromatic hydrocarbon (PAH)-degrading *Cycloclasticus* strains from the Gulf of Mexico and comparison of their PAH degradation ability with that of Puget Sound *Cycloclasticus* strains. Appl. Environ. Microbiol. 64, 4703–4710.
Goldthwait, S., Carlson, C., Henderson, G., Alldredge, A., 2005. Effects of physical fragmentation on remineralization of marine snow. Marine Ecol. Prog. Series 305, 59–65.
Gutierrez, T., Berry, D., Yang, T., Mishamandani, S., McKay, L., Teske, A., Aitken, M.D., 2013. Role of bacterial exopolysaccharides (EPS) in the fate of the oil released during the Deepwater Horizon oil spill. PLoS One 8, e67717.
Gutierrez, T., Rhodes, G., Mishamandani, S., Berry, D., Whitman, W.B., Nichols, P.D., Semple, K.T., Aitken, M.D., 2014. Polycyclic aromatic hydrocarbon degradation of phytoplankton-associated *Arenibacter* spp. and description of *Arenibacter algicola* sp. nov., an aromatic hydrocarbon-degrading bacterium. Appl. Environ. Microbiol. 80, 618–628.
Gutierrez, T., Teske, A., Ziervogel, K., Passow, U., Quigg, A., 2018. Microbial exopolymers: sources, chemico-physiological properties, and ecosystem effects in the marine environment. Front. Microbiol. 9, 1822.
Hamm, C.E., 2002. Interactive aggregation and sedimentation of diatoms and clay-sized lithogenic material. Limnol. Oceanograph. 47, 1790–1795.
Hazen, T.C., Dubinsky, E.A., DeSantis, T.Z., Andersen, G.L., Piceno, Y.M., Singh, N., Jansson, J.K., Probst, A., Borglin, S.E., Fortney, J.L., 2010. Deep-sea oil plume enriches indigenous oil-degrading bacteria. Science 330, 204–208.
ISO, 2016. ISO 10253 Water Quality — Marine Algal Growth Inhibition Test With *Skeletonema sp.* and *Phaeodactylum tricornutum*. International Organization for Standardization, Geneva, Switzerland.
Kamalanathan, M., Chiu, M.-H., Bacosa, H., Schwehr, K., Tsai, S.-M., Doyle, S., Yard, A., Mapes, S., Vasequez, C., Bretherton, L., 2019. Role of polysaccharides in diatom *Thalassiosira pseudonana* and its associated bacteria in hydrocarbon presence. Plant Physiol. 180, 1898–1911.
Katoh, K., Toh, H., 2010. Parallelization of the MAFFT multiple sequence alignment program. Bioinformatics 26, 1899–1900.
Kooistra, W.H., Sarno, D., Balzano, S., Gu, H., Andersen, R.A., Zingone, A., 2008. Global diversity and biogeography of *Skeletonema* species (Bacillariophyta). Protist 159, 177–193.
Kourafalou, V.H., Androulidakis, Y.S., 2013. Influence of Mississippi River induced circulation on the Deepwater Horizon oil spill transport. Journal of Geophysical Research: Oceans 118, 3823–3842.
Lee, K., Nedwed, T., Prince, R.C., Palandro, D., 2013. Lab tests on the biodegradation of chemically dispersed oil should consider the rapid dilution that occurs at sea. Mar. Pollut. Bull. 73, 314–318.
McFarlin, K.M., Prince, R.C., Perkins, R., Leigh, M.B., 2014. Biodegradation of dispersed oil in arctic seawater at-1 C. PLoS One 9, e84297.
McMurdie, P.J., Holmes, S., 2013. Phyloseq: an R package for reproducible interactive analysis and graphics of microbiome census data. PLoS One 8, e61217.
Messina, E., Denaro, R., Crisafi, F., Smedile, F., Cappello, S., Genovese, M., Genovese, L., Giuliano, L., Russo, D., Ferrer, M., 2016. Genome sequence of obligate marine polycyclic aromatic hydrocarbons-degrading bacterium *Cycloclasticus* sp. 78-ME, isolated from petroleum deposits of the sunken tanker Amoco Milford Haven, Mediterranean Sea. Mar. Genom. 25, 11–13.
Netzer, R., Henry, I.A., Ribicic, D., Wibberg, D., Brönner, U., Brakstad, O.G., 2018. Petroleum hydrocarbon and microbial community structure successions in marine oil-related aggregates associated with diatoms relevant for Arctic conditions. Mar. Pollut. Bull. 135, 759–768.
Nordtug, T., Olsen, A.J., Altin, D., Meier, S., Overrein, I., Hansen, B.H., Johansen, Ø., 2011. Method for generating parameterized ecotoxicity data of dispersed oil for use in environmental modelling. Mar. Pollut. Bull. 62, 2106–2113.
Passow, U., De La Rocha, C.L., 2006. Accumulation of mineral ballast on organic aggregates. Glob. Biogeochem. Cycles 20, GB1013.
Passow, U., Ziervogel, K., 2016. Marine snow sedimented oil released during the Deepwater Horizon spill. Oceanograp 29, 118–125.
Passow, U., Ziervogel, K., Asper, V., Diercks, A., 2012. Marine snow formation in the aftermath of the Deepwater Horizon oil spill in the Gulf of Mexico. Environ. Res. Lett. 7, 035301.
Passow, U., Sweet, J., Quigg, A., 2017. How the dispersant Corexit impacts the formation of sinking marine oil snow. Mar. Pollut. Bull. 125, 139–145.
Passow, U., Sweet, J., Francis, S., Xu, C., Dissanayake, A.L., Lin, Y.Y., Santschi, P.H., Quigg, A., 2019. Incorporation of oil into diatom aggregates. Mar. Ecol. Progr. Series 612, 65–86.
Piontek, J., Händel, N., Langer, G., Wohlers, J., Riebesell, U., Engel, A., 2009. Effects of rising temperature on the formation and microbial degradation of marine diatom aggregates. Aquat. Microb. Ecol. 54, 305–318.
Prince, R.C., Elmendorf, D.L., Lute, J.R., Hsu, C.S., Haith, C.E., Senius, J.D., Dechert, G.J., Douglas, G.S., Butler, E.L., 1994. 17. alpha.(H)-21. beta.(H)-hopane as a conserved internal marker for estimating the biodegradation of crude oil. Environ. Sci. Technol. 28, 142–145.
Prince, R.C., McFarlin, K.M., Butler, J.D., Febbo, E.J., Wang, F.C., Nedwed, T.J., 2013. The primary biodegradation of dispersed crude oil in the sea. Chemosphere 90, 521–526.
Quast, C., Pruesse, E., Yilmaz, P., Gerken, J., Schweer, T., Yarza, P., et al., 2013. The SILVA ribosomal RNA gene database project: improved data processing and web-

based tools. Nucleic Acids Res. 41, D590–D596.
Ribicic, D., McFarlin, K.M., Netzer, R., Brakstad, O.G., Winkler, A., Throne-Holst, M., Størseth, T.R., 2018a. Oil type and temperature dependent biodegradation dynamics-combining chemical and microbial community data through multivariate analysis. BMC Microbiol. 18, 83.
Ribicic, D., Netzer, R., Winkler, A., Brakstad, O.G., 2018b. Microbial communities in seawater from an Arctic and a temperate Norwegian fjord and their potentials for biodegradation of chemically dispersed oil at low seawater temperatures. Mar. Pollut. Bull. 129, 308–317.
Schroeder, P.J., Jenkins, D.G., 2018. How robust are popular beta diversity indices to sampling error? Ecosphere 9, e02100.
Siron, R., Pelletier, E., Brochu, C., 1995. Environmental factors influencing the biodegradation of petroleum hydrocarbons in cold seawater. Arch. Environ. Contam. Toxicol. 28, 406–416.
Stackebrandt, E., Goodfellow, M., 1991. Nucleic Acid Techniques in Bacterial Systematics. John Wiley and Sons, New York.
Størdal, I.F., Olsen, A.J., Jenssen, B.M., Netzer, R., Hansen, B.H., Altin, D., Brakstad, O.G., 2015. Concentrations of viable oil-degrading microorganisms are increased in feces from *Calanus finmarchicus* feeding in petroleum oil dispersions. Mar. Pollut. Bull. 98, 69–77.
Stout, S.A., Payne, J.R., 2016. Macondo oil in deep-sea sediments: part 1–sub-sea weathering of oil deposited on the seafloor. Mar. Pollut. Bull. 111, 365–380.
Stout, S.A., Rouhani, S., Liu, B., Oehrig, J., Ricker, R.W., Baker, G., Lewis, C., 2017. Assessing the footprint and volume of oil deposited in deep-sea sediments following the Deepwater Horizon oil spill. Mar. Pollut. Bull. 114, 327–342.
Techtmann, S.M., Zhuang, M., Campo, P., Holder, E., Elk, M., Hazen, T.C., Conmy, R., Santo Domingo, J.W., 2017. Corexit 9500 enhances oil biodegradation and changes active bacterial community structure of oil-enriched microcosms. Appl. Environ. Microbiol. 83, e03462-03416.
Teramoto, M., Ohuchi, M., Hatmanti, A., Darmayati, Y., Widyastuti, Y., Harayama, S., Fukunaga, Y., 2011. *Oleibacter marinus* gen. nov., sp. nov., a bacterium that degrades petroleum aliphatic hydrocarbons in a tropical marine environment. Int. J. System. Evolut. Microbiol. 61, 375–380.
Valentine, D.L., Fisher, G.B., Bagby, S.C., Nelson, R.K., Reddy, C.M., Sylva, S.P., Woo, M.A., 2014. Fallout plume of submerged oil from Deepwater Horizon. PNAS 111, 15906–15911.
Venosa, A., Holder, E., 2007. Biodegradability of dispersed crude oil at two different temperatures. Mar. Pollut. Bull. 54, 545–553.
Vonk, S.M., Hollander, D.J., Murk, A.J., 2015. Was the extreme and wide-spread marine oil-snow sedimentation and flocculent accumulation (MOSSFA) event during the Deepwater Horizon blow-out unique? Mar. Pollut. Bull. 100, 5–12.
Wirth, M.A., Passow, U., Jeschek, J., Hand, I., Schulz-Bull, D.E., 2018. Partitioning of oil compounds into marine oil snow: insights into prevailing mechanisms and dispersant effects. Mar. Chem. 206, 62–73.
Yakimov, M.M., Giuliano, L., Gentile, G., Crisafi, E., Chernikova, T.N., Abraham, W.-R., Lünsdorf, H., Timmis, K.N., Golyshin, P.N., 2003. *Oleispira antarctica* gen. nov., sp. nov., a novel hydrocarbonoclastic marine bacterium isolated from Antarctic coastal sea water. Int. J. System. Evolut. Microbiol. 53, 779–785.
Yakimov, M.M., Timmis, K.N., Golyshin, P.N., 2007. Obligate oil-degrading marine bacteria. Curr. Opin. Biotechnol. 18, 257–266.
Yergeau, E., Maynard, C., Sanschagrin, S., Champagne, J., Juck, D., Lee, K., Greer, C.W., 2015. Microbial community composition, functions, and activities in the Gulf of Mexico 1 year after the Deepwater Horizon accident. Appl. Environ. Microbiol. 81, 5855–5866.
Yu, Y., Lee, C., Kim, J., Hwang, S., 2005. Group-specific primer and probe sets to detect methanogenic communities using quantitative real-time polymerase chain reaction. Biotechnol. Bioeng. 89, 670–679.
Ziervogel, K., McKay, L., Rhodes, B., Osburn, C.L., Dickson-Brown, J., Arnosti, C., Teske, A., 2012. Microbial activities and dissolved organic matter dynamics in oil-contaminated surface seawater from the Deepwater Horizon oil spill site. PLoS One 7 (4).